Chinese Journal of Aeronautics, (2016), 29(2): 470–478

Chinese Society of Aeronautics and Astronautics
& Beihang University

Chinese Journal of Aeronautics

cja@buaa.edu.cn
www.sciencedirect.com

SNR periodical variation of Chang'E-3 spacecraft orbiting the Moon

He Qingbao *, Liu Qinghui, Li Peijia, Kawaguchi Noriyuki, Wu Yajun, Zheng Xin, Zhang Juan, Xu Zhijun

Shanghai Astronomical Observatory, Chinese Academy of Sciences, Shanghai 200030, China

Received 29 April 2015; revised 5 December 2015; accepted 7 January 2016
Available online 23 February 2016

KEYWORDS

2 bits quantization;
Elevation angle;
Moon radiation;
SNR periodical variation;
VLBI

Abstract Chang'E-3 spacecraft was orbiting the Moon from December 6–14, 2013, and very long baseline interferometry (VLBI) observations were performed to improve the accuracy of its orbit determination. In the process of recording VLBI raw data, 2 bits quantization was implemented. Interesting phenomenon was that signal-to-noise ratio (SNR) of each VLBI station experienced periodical change and had large variation on amplitude while in the Moon's orbit, whereas SNR kept in a stable level after Chang'E-3 landed on the Moon. Influence of varying elevation angle on SNR was analyzed and compensation of 2 bits quantization harmonics to SNR calculation was investigated. Most importantly, telescope system noise temperature increase caused by the Moon was computed along the time of Chang'E-3 orbiting the Moon, and well matched SNR changing trend in terms of correlation coefficients.

1. Introduction

With the advantage of short distance to earth, the Moon has been of interest for many space projects for better understanding the universe, such as well-known Apollo project, JAXA's SELenological and engineering explorer (SELENE/KAGUYA),[1] India's Chandrayaan-1,[2] etc. And China has just launched its third lunar spacecraft, Chang'E-3, on December 1, 2013, which went into the Moon's orbit on December 6, and then started orbiting the Moon in a two-hour polar orbit until it landed on the Moon on December 14, 2013. In the stage of orbiting the Moon, Chang'E-3 was first in a circular orbit (December 6–10) of 100 km in average altitude, and then entered into an elliptical orbit (December 10–14) with 15 km in perigee and 100 km in apogee. For the whole journey, very long baseline interferometry (VLBI) observations were performed, which involved telescopes of TianMa (TM:65 m), Beijing (BJ: 50 m), Kunming (KM: 40 m), and Urumqi (UR: 25 m), with the main purpose of improving the accuracy of its orbit determination.[3] Signal-to-noise ratio (SNR) of those received signals was calculated, and it kept in a stable level after landing on the Moon. However, at the time of orbiting the Moon, it experienced periodical change and had large variation on amplitude, which may affect the accuracy of engineering and scientific results, and on the other hand may carry

* Corresponding author. Tel.: +86 21 34775691.
E-mail address: qbhe@shao.ac.cn (Q. He).

Peer review under responsibility of Editorial Committee of CJA.

Production and hosting by Elsevier

http://dx.doi.org/10.1016/j.cja.2016.01.006
1000-9361 © 2016 Chinese Society of Aeronautics and Astronautics. Published by Elsevier Ltd.

scientific information. This paper mainly studies the reasons behind these variations.

SNR variations are attributed to changes in signal power or noise power, or both of them. Changes in noise power can be partly caused by the Moon, as the Moon radiates energy at microwave wavelengths and Chang'E-3 was flying near it. In previous studies,[4–6] a 34-m-diameter telescope experienced a system noise temperature increase about 189 K at X band (8.4 GHz) with antenna beam center pointed to the Moon disk center and it was discovered that with antenna beam center pointing to the Moon center, antenna system noise temperature would increase more if the beam is sharper, and if the beam center gradually points away from the Moon center, antenna system noise temperature will decrease.[7] With actual data of Chang'E-3, this paper highlights the relation between SNR variation and system noise temperature increase due to the Moon.

In Section 2, we introduce the methods of obtaining SNR and present the results of both at the time of orbiting the Moon and after landing on the Moon. In Section 3, we mainly analyze SNR variation at the time of orbiting the Moon from aspects of elevation angle, 2 bits quantization harmonics and telescope system noise temperature increase due to the Moon. In Section 4, some other reasons for SNR variation are discussed and nonuniform brightness temperature T_b distribution is mentioned. Time in this paper is in coordinated universal time (UTC).

2. SNR acquisition

2.1. Signal flow

While ground radio telescopes were used to observe Chang'E-3, signal flow inside telescopes was as Fig. 1 shows (ADC means Analog-to-digital converter; AGC means automatic gain control). Raw data of VLBI were recorded by 2 bits, whose influence on SNR calculation will be analyzed in Section 3.2, and then transmitted to Shanghai VLBI center via communication network for further processing.

2.2. SNR calculation methods and results

As supported by Shanghai VLBI center, we calculated SNR values of the 4 stations, individually, both at the time of orbiting the Moon and after landing on the Moon.

When Chang'E-3 was orbiting the Moon, it transmitted differential one-way range (DOR) signals with carrier frequency f_c of 8470 MHz. We picked up the carrier channel (2 MHz bandwidth) and implemented the following methods to calculate SNR.

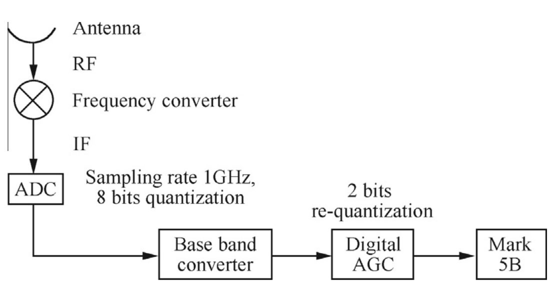

Fig. 1 Signal flow of VLBI stations.

First, obtain the auto-correlation power, and sum up all the values, labeled as P. Second, fit noise power, and sum up all the fitted values, labeled as P_n. Third, SNR = $(P - P_n)/P_n$. Fig. 2(a) gives an example of auto-correlation power of DOR carrier channel and noise fit result, from TM station, December 9, 2013. In Fig. 2(a), ($f_c \pm 65$ kHz) are telemetry signals, ($f_c \pm 500$ kHz) are range tones, and other lower peaks are higher harmonics of telemetry signal.

It should be noted that we didn't calculate SNR of single carrier frequency, because there were fence effect and power leakage in the process of doing fast Fourier transform (FFT). As a result, SNR of single carrier frequency departed from its true values and varied in the same manner as Doppler shift frequency variation. However, the above methods avoided these undesired effects and SNR calculation results of December 9, 2013 are shown in Fig. 3.

In Fig. 3, there are some gaps in SNR values. The big gaps (around 1 h) were caused by Chang'E-3 flying to the far side of the Moon, and the small gaps (around 5 min) were caused by telescopes directed to radio sources for VLBI calibration. An interesting phenomenon is that SNR changes periodically around every two hours, and has large amplitude variation. We have not seen this phenomenon in other papers, although this may also apply to other lunar orbiters.

To better understand this phenomenon, SNR after Chang'E-3 landed on the Moon was necessary to be calculated, and to serve as a reference. After Chang'E-3 landed on the Moon, it separated into a rover and a lander. The lander continuously sent data transmission signals for about 10 h a day at center frequency of 8496 MHz and bandwidth of 5 MHz (Fig. 2(b)).[3] We used the peak point (A) and trough point (B) to calculate its SNR, and results of December 23, 2013 are shown in Fig. 4, in which the time after 24 h represents early morning of December 24, 2013.

3. SNR variation analysis

Compared with SNR after landing on the Moon (Fig. 4), SNR of orbiting the Moon (Fig. 3) experienced more complicated variations. In Fig. 3, TM had the largest variation of about 8 dB, while other three stations suffered more or less 5 dB, and they had periodical change of around 2 h. It was unlikely to be caused by the attitude of the orbiter, because antenna on the orbiter was with effective isotropic radiated power (EIRP) of 0 dBw for 80% of radiating direction, and of −3 dBw for the rest of 20%. It is the main purpose of this study to know the reasons and information behind those variations. However, individual investigation on noise power variation or signal power variation was not feasible, because digital AGC unit was introduced in the signal flow (Fig. 1), which kept the total power as a constant. In this chapter, we analyze SNR variation of orbiting the Moon from aspects of elevation angle, 2 bits quantization harmonics, and radiation energy from the Moon. SNR after landing on the Moon is mainly served as a reference and its variation is analyzed only in Section 3.1.

3.1. Elevation angle

After Chang'E-3 landed on the Moon, the lander was in a fixed position. And as one can see in Fig. 4, SNR of TM and BJ are stable with time, while SNR of KM and UR have some

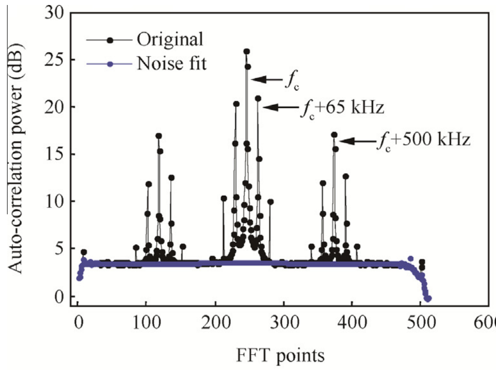

(a) December 9, 2013
(Bandwidth is 2 MHz, half FFT size is 512)

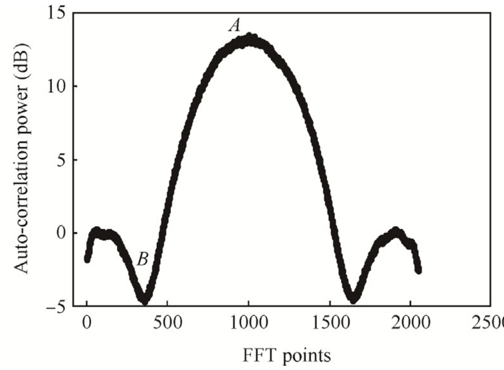

(b) December 23, 2013
(Bandwidth is 8 MHz, half FFT size is 2048)

Fig. 2 Auto-correlation power from TM station.

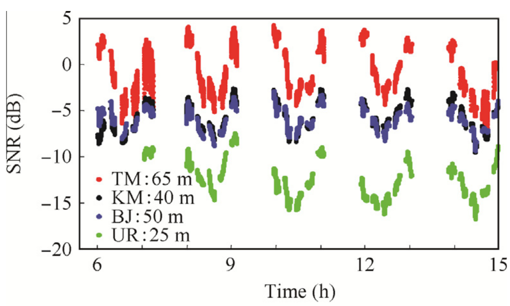

Fig. 3 SNR of main carrier channel of DOR signals on December 9, 2013.

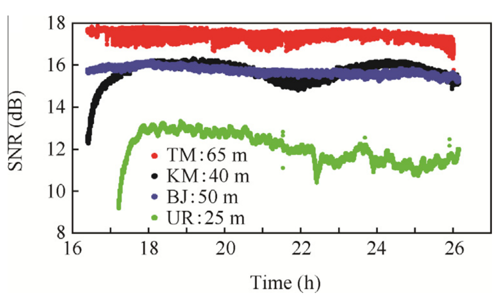

Fig. 4 SNR of data transmission signals from lander on December 23–24, 2013.

changes. SNR of KM has a wave-like change. This is closely related to its elevation angle which is shown in Fig. 5(a). It is well known that antenna efficiency is low with small elevation angle, and it increases as elevation angle goes up to a certain point, which depends on its telescope design and is usually between 40° and 50°, then it decreases as elevation angle further increases. Except this, when elevation angle is small, antenna noise temperature is big due to atmosphere and ground reflection. This also explains why SNR of UR in Fig. 4 increases at the beginning part. But it's strange that SNR of UR shows some turbulence after 18 h and decreases as elevation angle goes up. Investigation result shows that this is due to a high mountain in the south-west direction of UR station, and it caused unstable increase on antenna system noise temperature as telescope tracking Chang'E-3 at the Moon's orbit. From the above analyses, we can conclude that transmitting power from the lander was stable, and it is reasonable to assume that the transmitting power at the time of orbiting the Moon had the same performance.

At the time of orbiting the Moon, elevation angle variation also affected SNR values. Fig. 5(b) shows elevation angle of 4 stations on December 9, 2013. Elevation angle was small when telescopes of UR and KM started observing Chang'E-3. And it resulted in relatively small SNR values (Fig. 3). At the last phase of observing at the day, elevation angles of TM and BJ decreased to a small value, which resulted in decrease of SNR values (Fig. 3). For UR station, the overall trend of SNR was decreasing (Fig. 3), which was also due to a high mountain near UR station.

3.2. SNR compensation for 2 bits quantization harmonics

When Chang'E-3 was orbiting the Moon, SNR experienced periodical change (Fig. 3). With the intention of better understanding, influence of quantization harmonics on SNR calculation needs to be considered.

After signals were received by telescopes, they went through 8 bits quantization and 2 bits re-quantization processes (Fig. 1). Theoretical sensitivity factor for 2 bits quantization is 0.8818,[8] while for 8 bits is 0.9999,[9] which equal SNR loss of 0.55 dB and 4×10^{-4} dB, respectively. In actual calculation of SNR, not just theoretical loss happened, but also part of quantization harmonics was covered by noise and treated as noise in auto-correlation power spectrum in the case of strong SNR. As a result, calculated SNR would be smaller than theoretical ones. Since 8 bits quantization has 255 quantization levels, power distributed to quantization harmonics would be small enough to neglect. This study only considers compensation to SNR due to 2 bits quantization harmonics. To know the compensation values, simulations were made.

In simulations, the general thought was first recording SNR before 2 bits quantization and then calculating SNR after it, then obtaining the difference between them. Under this thought, we considered 3 different situations. The first one was random noise impressed on a sine-wave signal, with noise power in a fixed value, for example 0.01 W and SNR changed from −26.5 dB to 10 dB at step of 1 dB. The second one was

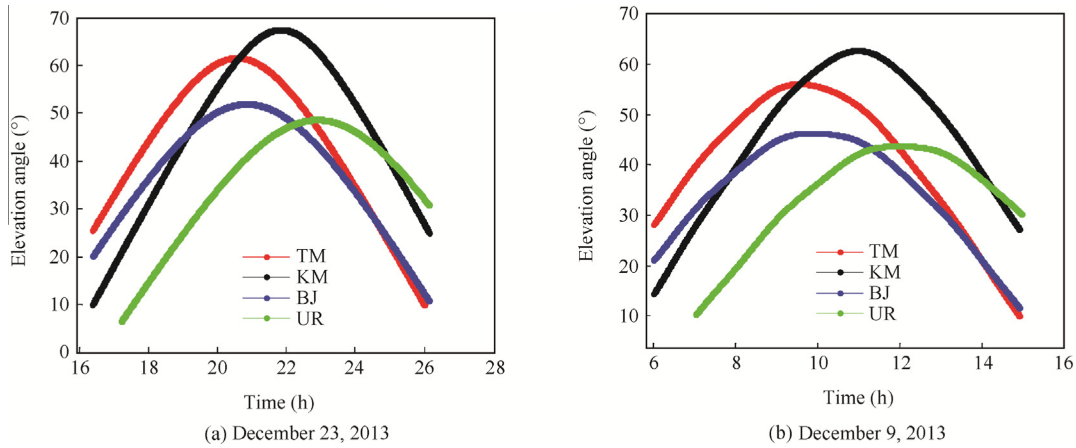

Fig. 5 Elevation angle of telescopes on December 9, 2013 and December 23, 2013.

similar with the above. Differences were power of sine-wave signal was in a fixed value, while noise power was not, and SNR was set from −25 dB to 10 dB. The third one was random noise impressed on a modulated signal, and others were the same with the second one. Table 1 gives an inventory of these three situations. As one can see in Table 1, either signal power P_s or random noise power σ was unfixed, and their values could be calculated by utilizing SNR and fixed σ or P_s.

In actual cases, signal frequency received by telescopes varied with time due to Doppler shift frequency. To meet the general situation, we set f = 0.9375 MHz in Table 1. And for the third situation, the purpose was to know whether there is any difference between sine-wave signal and modulated signal, and we set f_1 = 78.125 kHz.

When performing simulations, for each situation, we first sampled signals with sampling rate 4 MHz and recorded SNR, then quantified signals with 2 bits, and finally performed FFT algorithm for every 1024 samplers and obtained auto-correlation power spectrum with integration time of one second. These parameters were in accord with those which were used in processing Chang'E-3 DOR signals. Fig. 6 gives an example of auto-correlation power spectrum of the third situation, with SNR before quantization as 8 dB. In Fig. 6, the sign of all signals includes obvious quantization harmonics while the sign of signal doesn't. Based on this, we calculated SNR and Fig. 7 (a) shows the results of the third situation.

In Fig. 7(a), curves of all signals and signal represent SNR with and without considering obvious quantization harmonics as signals. Line of theory is theoretical values, which equal SNR before quantization minus 0.55 dB. As one can see that curve of all signals and curve of signal are extremely close and both are below line of theory when SNR before 2 bits quantization is bigger than around 2 dB. This indicates those obvious quantization harmonics accounts for only a small part

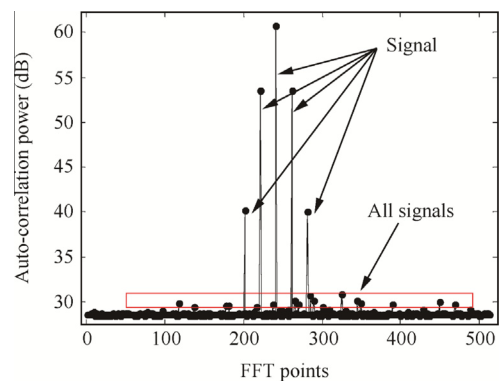

Fig. 6 Auto-correlation power spectrum of the third situation with SNR as 8 dB.

of all the harmonics, and there were a lot more which were not picked up and covered by noise. To have a clear view of the difference between theoretical values and calculated ones, subtraction operation was performed between line of theory and curve of all signals for each situation, and results are shown in Fig. 7(b).

Fig. 7(b) shows very similar results for the 3 situations, and we didn't detect any obvious difference between the first (or second) situation and the third situation. Some turbulence happened in the second and third situation at the start because quantization level was calculated with low accuracy in the case of extremely big noise power. The green curve in Fig. 7(b) is fit results of average values of the 3 situations. It is first close to zero, then slightly smaller than zero, and finally much bigger than zero as SNR before quantization changes from −26.5 to 10 dB. This can be explained as follows: when SNR is very small, for example −25 dB, there is no quantization harmonics and noise suppression effect when adopting 2 bits

Table 1 Three different situations considered in simulations.

Situation No.	Set SNR	Signal expression	Signal power	Random noise
1	−26.5–10 dB	$\sqrt{2P_s}\sin(2\pi ft)$	P_s unfixed	σ = 0.01
2	−25–10 dB	$\sqrt{2P_s}\sin(2\pi ft)$	P_s = 0.01	σ unfixed
3	−25–10 dB	$\sqrt{2P_s}\sin[2\pi ft + 0.8\sin(2\pi f_1 t)]$	P_s = 0.01	σ unfixed

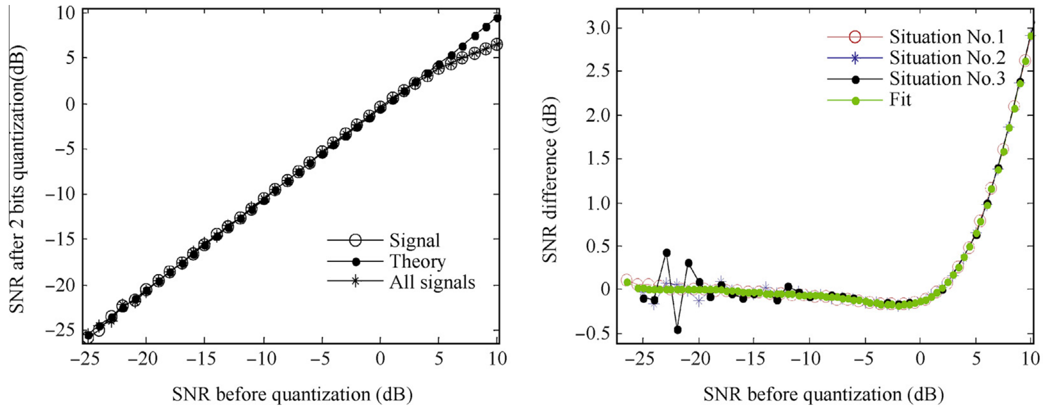

(a) SNR values before and after 2 bits quantization (b) Difference between calculated SNR and theoretical ones

Fig. 7 SNR values before and after 2 bits quantization of the third situation and SNR difference between calculated SNR and theoretical one's.

quantization, so SNR values should be equal to theoretical ones, then SNR difference should be zero; when SNR becomes bigger, like −2 dB, quantization harmonics and noise suppression effect both appear, and noise suppression effect is predominant; when SNR continues to increase, like 5 dB, quantization harmonics become more severe than noise suppression.

From the simulation results, we first compensated for the influence of 2 bits quantization harmonics on calculated SNR. And then we recovered SNR before 2 bits quantization by plus 0.55 dB, which is theoretical SNR loss of 2 bits quantization. Results are shown in Fig. 8.

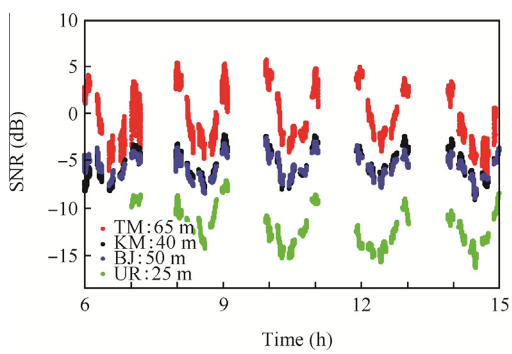

Fig. 8 SNR before 2 bits quantization on December 9, 2013.

3.3. Influence of Moon's radiation energy on SNR

After compensating for SNR loss due to 2 bits quantization at the time of Chang'E-3 orbiting the Moon, periodical change on SNR still exists and SNR of TM varies even in a bigger scale on amplitude, comparing Fig. 3 with Fig. 8. This phenomenon could not be caused by signal flow inside telescopes (Fig. 1), because they were very small and were ignored in this study. It is reasonable to associate this phenomenon with radiation energy from the Moon, because the Moon was also observed as telescopes were pointing to Chang'E-3 at the time of orbiting the Moon (Fig. 9). And it is well known that the Moon radiates energy at microwave wavelengths, and noise power is proportional to noise temperature. As telescopes tracking Chang'E-3, radiation energy from the Moon which entered telescopes' beam may vary with time. As a consequence, telescopes would experience an increase on its

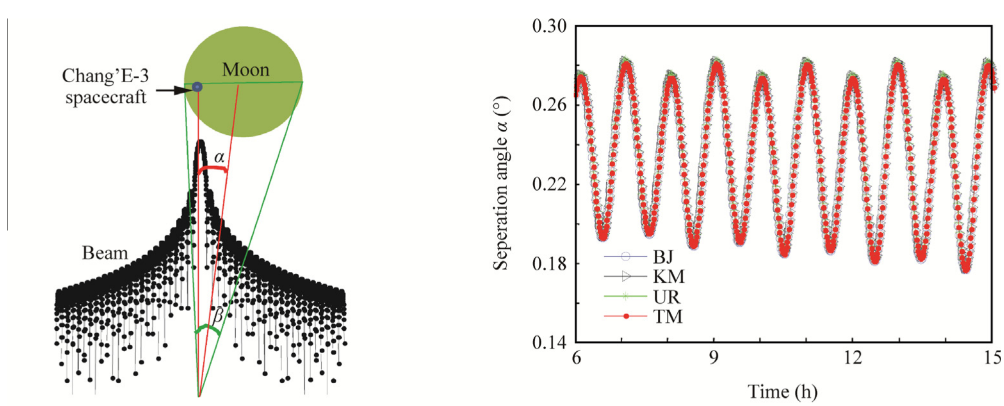

(a) Sketch of a telescope observing Chang'E-3 (b) Separation angle of Chang'E-3 and the Moon center

Fig. 9 Sketch of a telescope observing Chang'E-3 when it was orbiting the Moon and separation angles of Chang'E-3 and the Moon center from the view of telescopes' site on December 9, 2013.

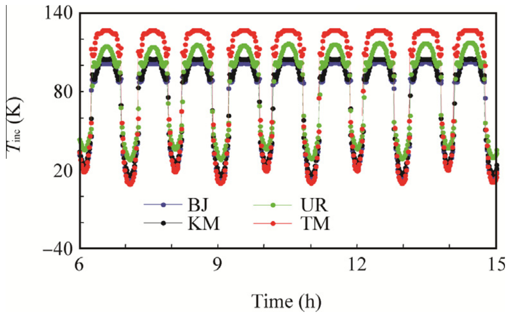

Fig. 10 System noise temperature increase due to the Moon (December 9, 2013).

system noise temperature,[6] and its value may vary with time. In Fig. 9(a), a sketch of telescope observing Chang'E-3 when it was orbiting the Moon is given; α represents the separation angle of viewing Chang'E-3 and the Moon center from a telescope site, which corresponds to the values in Fig. 9(b), and β is the angle of the Moon disk ($\beta \approx 0.5°$). To have an overall scale view, the separation angles of Chang'E-3 and the Moon center were also computed when telescopes were pointing to radio sources and Chang'E-3 flew to the far side of the Moon. As shown in the right side of Fig. 9, the separation angles have a stable periodical change, which would result in periodical variation in telescopes system noise temperature and thus affect SNR.

The Moon's radiation energy at a certain frequency is measured by brightness temperature T_b. To compute system noise temperature increase T_{inc} (unit Kelvin) due to the Moon, we used the following expression[7]

$$T_{inc} = \frac{\int_{Moon} G(\theta, \phi) T_b(\theta, \phi) d\Omega}{\int_{4\pi} G(\theta, \phi) d\Omega} \times \eta \tag{1}$$

where $G(\theta, \phi)$ is normalized gain pattern of telescope, θ and ϕ are elevation and azimuth angle, $T_b(\theta, \phi)$ is brightness temperature of the Moon in direction of (θ, ϕ), unit Kelvin, and η is antenna efficiency (BJ:45%, KM:47%,[10] UR:54%,[11] TM:55%[12]).

In previous studies, global T_b distribution at frequency of 7.8 GHz has been worked out with data from the second Chinese lunar spacecraft Chang'E-2.[13] However, high resolution of T_b distribution on the Moon at frequency of 8470 MHz (DOR carrier frequency of Chang'E-3) remains unknown. Knowing that the local time of Chang'E-3 flying track on the front side of the Moon on December 9, 2013 was daytime, we assumed T_b as 240 K all over its observing track based on the study of Fang & Fa.[13]

Before computing T_{inc}, normalized gain pattern for each telescope is assumed as[7]

$$G(\theta, \phi) = \left(\frac{2\lambda}{\pi D} \frac{J_1 \left[\frac{\pi D}{\lambda} \sin\theta \right]}{\sin\theta} \right)^2 \tag{2}$$

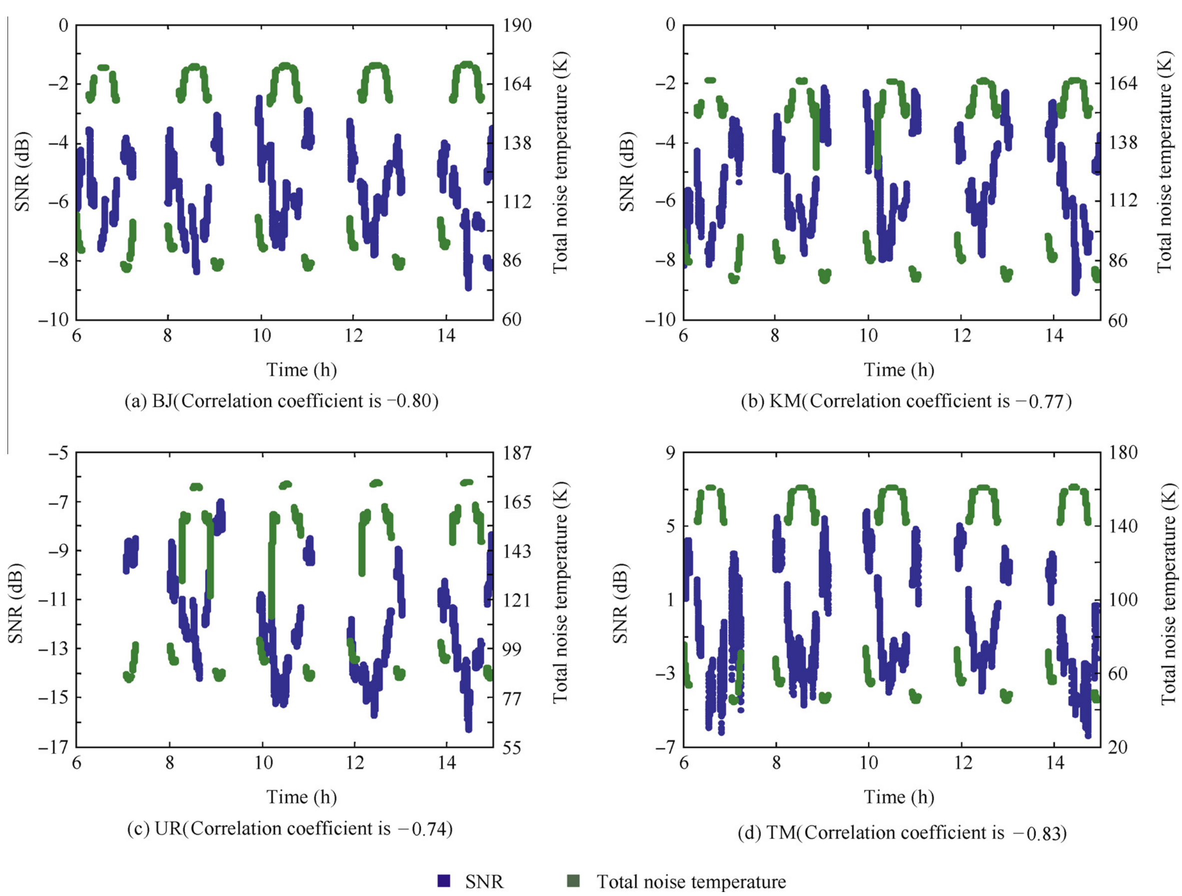

Fig. 11 SNR and total noise temperature of 4 stations on December 9, 2013 and their correlation coefficients.

where D is diameter of telescope (BJ:50 m, KM:40 m, UR:25 m, TM:65 m), λ wavelength of DOR carrier frequency ($\lambda \approx 3.54$ cm), and J_1 the first order of Bessel function. Utilizing the values of separation angle in Fig. 9 and Eqs. (1) and (2), values of T_{inc} due to the Moon are computed (Fig. 10).

To have an overall scale view of its changing trend, values of T_{inc} were computed continuously in time in Fig. 10, in accord with separation angle in Fig. 9(b). With different telescope size and efficiency, values of T_{inc} differ among stations in Fig. 10. As one can see, values of T_{inc} are with clear periodical variation of around two hours, and change rapidly as beam center is close to the Moon's edge. These phenomena correspond to the facts that orbit period of Chang'E-3 was around 2 h and antenna beam energy mostly focused on main beam, which is very sharp in X-band frequency. T_{inc} of TM has the largest variation scale, with maximum 128 K and minimum 6 K, which would result in considerable change of its SNR.

Ground radio telescopes have their own system noise temperature T_{sys}, and SNR is directly affected by the combination of T_{sys} and T_{inc}. We calculated total noise temperature T_{total} by plus average T_{sys} (BJ:70 K,[14] KM:61 K, UR:57 K,[11] TM:35 K[12]) and T_{inc}, then calculated correlation coefficients between SNR and T_{total} (Fig. 11).

In Fig. 11, correlation coefficients are from −0.74 to −0.83, which indicate that SNR and T_{total} are well matched in the opposite way, and demonstrate that T_{inc} caused by the Moon was the main reason for SNR varying so largely and periodically. UR had the worst correlation coefficient mainly because the noise temperature caused by the nearby high mountain was not accounted. And BJ had better correlation coefficient than KM probably because elevation angle of KM varied in larger scale than BJ. TM had the best correlation coefficient due to a joint effort of the lowest T_{sys} of TM and the largest variation of T_{inc}. This also explains why SNR of TM in Fig. 8 varies in the biggest scale.

4. Discussion

After zooming in the values of SNR and T_{total} (Fig. 12), we found T_{total} was not changing in the exactly opposite way with SNR. In Fig. 12, it's most obvious during the time of 12.4–12.6 h. This is in accord with imperfect correlation coefficients in Fig. 11. Reasons can be concluded as follows: first, T_{sys} of ground telescopes suffered variation due to varying elevation angle and thermal radiation from surrounding environment, as analyzed in Section 3.1; second, gain of ground telescopes

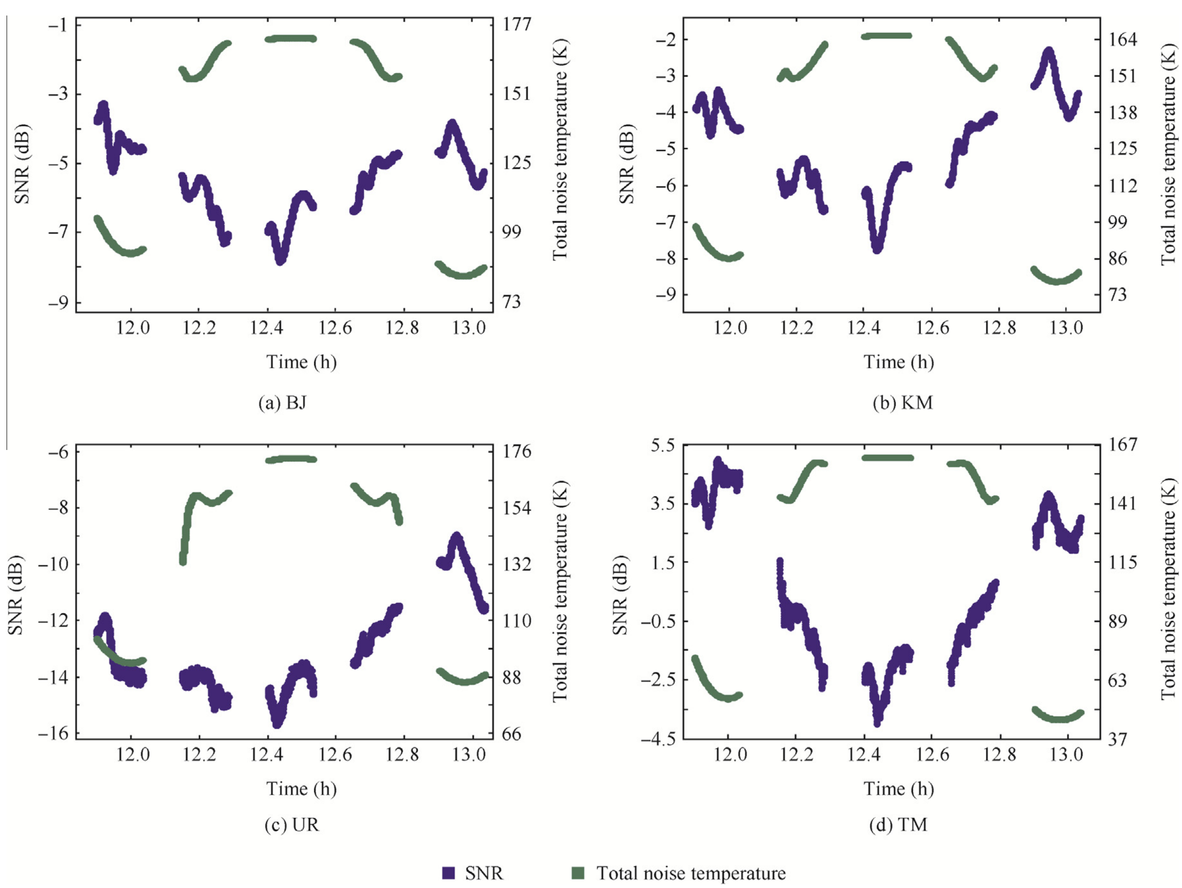

Fig. 12 Zooming in values of SNR and total noise temperature on December 9, 2013.

also slightly changed with varying elevation angle, and in computing system noise temperature increase due to the Moon, approximated antenna gain pattern was implemented instead of actual one's; third, transmitting power from Chang'E-3 may have some slight variation; fourth, T_b was assumed as a fixed value in computation, while actual T_b varies with locations.[13] Obtaining the above parameters with higher accuracy is challenging, and it would be a future work. Here we mention effect on SNR from nonuniform T_b distribution on the Moon.

In Fig. 12, within the time of 12.4–12.6 h, SNR first drops and then increases, while calculated T_{total} was almost flat. Large variation on transmitting power from Chang'E-3 is not likely to be the reason, for SNR values are almost the same in neighboring orbit periods (Fig. 11). Changes in T_{sys} by varying elevation angle and surrounding environment also fail to explain it, because telescopes only changed their directions within a tiny level in a short time. From research of Fang & Fa, we know T_b distribution on the Moon at 7.8 GHz (Fig. 13).[13] It can almost represent features of T_b at 8470 MHz, which is DOR carrier frequency of Chang'E-3, due to small difference between their wavelengths. To better understand the SNR variation, we marked Chang'E-3 flying track during 12.4–12.6 h on December 9, 2013 using red arrow and red dash line in Fig. 13, and drew main beam size of KM at frequency of 8470 MHz in black dashed circle. It should be noted that main beam size of UR is bigger than KM, while for BJ and TM, it is smaller, due to their telescopes' sizes. Radiation energy from the main beam area accounts for most part of the total radiation energy from the Moon which was received by ground telescopes. As we can see, within red dash line, T_b first increases and then decreases, and it is reasonable to think this might be one of the factors which caused SNR variation during the corresponding time in Fig. 12. The attitude of the orbiter and lunar surface reflection may also contribute to SNR minor variation.

With variation on SNR, random error on DOR group delay also changes. For SNR of carrier frequency (just one spectral line) is as high as around 20 dB,[15] when SNR drops 5 dB due to Moon's radiation, random error of DOR group delay becomes 0.1 ns larger. But when ground telescopes direct to the edge of the Moon, SNR drops less than 5 dB. So over all, for the Moon's orbiter, using baseline length of 2000 km, we estimate that it causes a few meters error on orbit determination. But in case SNR of carrier frequency goes lower, and then SNR drops 5 dB due to the Moon's radiation, it will cause larger error on DOR group delay and orbit determination.

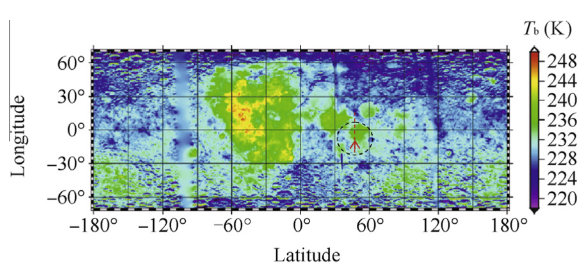

Fig. 13 T_b distribution over lunar surface at noon for 7.8 GHz.[13]

5. Conclusions

SNR periodical variation at the time of Chang'E-3 orbiting the Moon is mainly caused by the variation of the radiation energy from the Moon which is received by ground telescopes. Contributing factors for SNR minor variation includes varying elevation angle of telescopes, thermal radiation from surrounding environment and nonuniform T_b distribution on lunar surface. For SNR calculation, 2 bits quantization harmonics makes it smaller than theoretical one if SNR is bigger than around 2 dB.

Acknowledgements

The authors thank people working in Shanghai VLBI center who provided data for this work. This work was supported by the National Natural Science Foundation of China (Nos. 11473059, 11273049, 11403082).

References

1. Kato M, Sasaki S, Tanaka K, Lijima Y, Takizawa Y. The Japanese lunar mission SELENE: Science goals and present status. *Adv Space Res* 2008;**42**(2):294–300.
2. Goswami J, Annadurai M. Chandrayaan-1: India's first planetary science mission to the Moon. *Curr Sci* 2009;**96**(4):486–91.
3. Liu QH, Zheng X, Huang Y, Li PJ, He QB, Wu YJ, et al. Monitoring motion and measuring relative position and Chang'E-3 rover. *Radio Sci* 2014;**49**:1080–6.
4. Morabito DD, Imbriale W, Keihm S. Observing the Moon at microwave frequencies using large-diameter deep space network antenna. *IEEE Trans Antenna and Propag* 2008;**56**(3):650–60.
5. Morabito DD. Lunar noise-temperature increase measurements at S-band, X-band, and Ka-band using a 34-meter-diameter beam-waveguide antenna. Pasadena, California: Jet Propulsion Laboratory; 2006. p. 1–18. Inter Planetary Report (IPN) Progress Report 42–166.
6. Imtriale WA. Computing the noise temperature increase caused by pointing DSS 13 at the center of Moon. Pasadena, California: Jet Propulsion Laboratory; 2006. p.1–10. Inter Planetary Report (IPN) Progress Report 42–166.
7. Ho C, Kantak A, Slobin S, Morabito DD. Link analysis of a telecommunication system on earth, in geostationary orbit, and at the Moon: Atmospheric attenuation and noise temperature effects. Pasadena, California: Jet Propulsion Laboratory; 2007. p. 1–22. Inter Planetary Report (IPN) Progress Report 42–168.
8. Felli M, Spencer RE. *Very long baseline interferometry-techniques and applications*. The Netherlands: Kluwer Academic Publishers; 1989. p. 30–40.
9. Xiang Y. Research on digital base-band converter in VLBI data acquisition terminal [dissertation]. Shanghai: Shanghai Astronomical Observatory, Chinese Academy of Sciences; 2005 [Chinese].
10. Zhang HB, Mao PF, Wang M, Zhou JJ, Zhu XY, Shi SB. The 40 m Radio telescope. *Astron Res Technol* 2008;**5**(2):187–91 [Chinese].
11. Liu X, Song HG, Chen CY. Antenna patameters measurements in summer 2007. p. 1–27. Urumqi, China: Xinjiang Astronomical Observatory; 2007. Xinjiang Astronomical Observatory 25 m radio telescope Technical report 1[Chinese].
12. Wang JQ, Yu LF, Zhao RB, Dong J, Zuo XT, Gou W, et al. Sub-reflector model depending on elevations and performance evaluation for TM65 m radio telescope. *Sci Sin Phys Mech Astron* 2014;**44**(11):1232–40 [Chinese].
13. Fang T, Fa WZ. High frequency thermal emission from the lunar surface and surface of the Moon from Chang'E-2 Microwave radiometer. *Icarus* 2014;**232**:34–53.

14. Zhang XZ, Zhu XY, Kong DQ, Zheng L, Yao C, Zhang HB, et al. Measurements of electronic properties of the Miyun 50 m radio Telescope. *Res Astron Astrophys* 2009;**9**(3):367–76.
15. Liu QH, He QB, Zheng X, Wu YJ, Li PJ, et al. Analysis of VLBI observation for Tianma radio telescope in Chang'E-3 orbit determination. *Sci Sin Phys Mech Astron* 2015;**45**(3), 039501-1-9 [Chinese].

He Qingbao is a Ph.D. student at Shanghai Astronomical Observatory, Chinese Academy of Sciences. He received the B.S. degree in electronic engineering from Zhejiang A&F University in 2011. His main research interests are deep space exploration and VLBI phase delay.

Liu Qinghui is a professor and Ph.D. supervisor at Shanghai Astronomical Observatory, Chinese Academy of Sciences. He received the Ph.D. degree from Kagoshima University in 2003. His current research interests are VLBI techniques, deep space exploration, and atmospheric disturbances.